

# Analysis of Perovskite ( $\text{CH}_3\text{NH}_3\text{PbI}_3$ ) Solar Cells Using $\text{Cu}_2\text{O}$ as a Hole Transport Layer (HTL) With Varying ETL Thickness

Surendra Yadav<sup>1,\*</sup>, Ravi Shankar Yadav<sup>2</sup>

## Abstract

Solar cells offer a viable option for creating new clean energy solutions, though they may require supplementary energy sources. Renewable electricity sources, known for being affordable, accessible, and greenhouse gas-free, are increasingly popular. Photovoltaic cells, which convert sunlight into electricity, stand out as an excellent choice. Over the past two decades, advancements in photovoltaic technology have significantly reduced costs and enhanced the efficiency of solar cells. Perovskite materials, recognized for their unique crystal structure and versatile properties, hold particular promise for solar energy applications. The hole transport layer (HTL) is vital for the efficiency of solar cells using perovskite materials such as  $\text{CH}_3\text{NH}_3\text{PbI}_3$ . Simulation software like the SCAPS Tool has demonstrated the importance of the HTL in these cells. Quantitative simulations and models have been employed to ascertain the electrical properties of the  $\text{MAPbI}_3$  material in the active layer. These studies focus on parameters like fill factor (FF), short-circuit current density ( $J_{sc}$ ), power conversion efficiency (PCE), and open-circuit voltage ( $V_{oc}$ ). Additional calculations have been conducted for the capacitance-frequency (C-F) and capacitance-voltage (C-V) characteristics of previously studied perovskite solar cells. Simulation results indicate the performance of  $\text{MAPbI}_3$  with varying ETL thicknesses. For instance, at an ETL thickness of 0.020, the cells exhibited, FF = 41.69%, PCE = 30.95%,  $V_{oc}$  = 2.79V,  $J_{sc}$  = 26.53 mA/cm<sup>2</sup>, at an ETL thickness of 0.030, the cells exhibited, FF = 41.62%, PCE = 30.93%,  $V_{oc}$  = 2.80V,  $J_{sc}$  = 26.48 mA/cm<sup>2</sup>, at an ETL thickness of 0.040, the cells exhibited, FF = 41.60%, PCE = 30.95%,  $V_{oc}$  = 2.80V,  $J_{sc}$  = 26.48 mA/cm<sup>2</sup>.

**Keywords:** Perovskite solar cell,  $\text{CH}_3\text{NH}_3\text{PbI}_3$ ,  $\text{Cu}_2\text{O}$ , C-f, C-V, FF,  $V_{oc}$ ,  $J_{sc}$ , and PCE

## INTRODUCTION

Solar cells present a practical solution that may sometimes need additional energy sources to advance new clean energy technologies. Renewable electricity is valued for its affordability, accessibility, and lack of greenhouse gas emissions. Photovoltaic cells, which convert sunlight into electrical power, are a promising option for this purpose.

### \*Author for Correspondence

Surendra Yadav  
E-mail: syap5474@gmail.com

<sup>1</sup>M. Tech Scholar, Department of Electronics & Communication Engineering, Goel Institute of Management and Technology, Lucknow, Uttar Pradesh, India

<sup>2</sup>Associate Professor, Department of Electronics & Communication Engineering, Goel Institute of Management and Technology, Lucknow, Uttar Pradesh, India

Received Date: June 19, 2024

Accepted Date: July 23, 2024

Published Date: July 30, 2024

**Citation:** Surendra Yadav, Ravi Shankar Yadav. Analysis of Perovskite ( $\text{CH}_3\text{NH}_3\text{PbI}_3$ ) Solar Cells Using  $\text{Cu}_2\text{O}$  as a Hole Transport Layer (HTL) With Varying ETL Thickness. Journal of Nuclear Engineering & Technology. 2024; 14(2): 38–48p.

Over the last two decades, various material innovations have driven significant advancements in photovoltaic technology, reducing costs and improving solar cell efficiency [1]. The first efficient photovoltaic system was developed by Bell Laboratories in 1954, achieving 6% efficiency. Silicon solar panels, with a band gap of around 1 eV, are known for their high efficiency.

Lightweight film solar cells offer benefits due to their low weight and flexibility. Third-generation

solar cells incorporate materials such as organic dyes, conductive polymers, and silicon wires, which have larger band gaps [2]. These developments are critical for the future of renewable energy sources, as photovoltaic cells can provide a continuous supply of energy without emitting carbon dioxide.

Sustainable energy can be harnessed from natural resources like sunlight, tides, wind, and rain. Solar energy, in particular, is safe and advantageous for health, residential, and commercial use. Looking ahead, solar cells have the potential to become the primary source of renewable energy.

Solar power stands out as the most reliable and stable source of free energy. Among the various materials being explored to enhance this technology [3], elements within the perovskite family show significant promise. Copper Iodide (CuI) is particularly advantageous due to its chemical stability, ease of synthesis, and high transparency in the visible spectrum. However, using Deep Eutectic Solvents (DES) to process CuI can cause degradation of the perovskite layer.

Researchers have explored CuI-based perovskite solar cells [4] (PSCs) with p-in configurations. In 2015, Ye et al. demonstrated a method for rapidly depositing and crystallizing a CH<sub>3</sub>NH<sub>3</sub>PbI<sub>3</sub> film (with halides X = I, Br, and Cl) on an electrodeposited CuI layer. This approach achieved an average power conversion efficiency (PCE) of 15%, with a peak PCE of 16.6%. CuI-based PSCs had a success rate of 6%, likely due to the high hole mobility of the CuSCN hole transport layer (HTL).

The low interface resistance and smoothness of the perovskite films contributed to this performance [5]. Researchers have also used unconventional methods to create the perovskite layer.

Investigations have focused on the effectiveness of the HTL in CH<sub>3</sub>NH<sub>3</sub>PbI<sub>3</sub> (X = I) solar cells made from perovskite and inorganic cuprous oxide (Cu<sub>2</sub>O). A solar cell [6], also known as a photovoltaic cell, directly converts sunlight into electricity through the photovoltaic effect. Here is a simplified explanation of how a solar cell works [2].

## HOW A SOLAR CELL WORKS

### Light Absorption

When sunlight hits the solar cell, the perovskite layer absorbs photons (light particles). This energy excites electrons in the perovskite material, creating electron-hole pairs.

### Charge Separation

The excited electrons move to the conduction band, leaving behind holes in the valence band. The HTL (Cu<sub>2</sub>O or CuI) facilitates the movement of holes while the electron transport layer (ETL) collects the electrons.

### Charge Collection

The electrons travel through the ETL to the external circuit, generating an electric current. Meanwhile, the holes move through the HTL to the opposite electrode.

### Electric Power Generation

The movement of electrons through the external circuit creates a flow of electricity, which can be used to power electrical devices or stored in batteries.

Essentially, a solar cell is a sustainable and renewable source of electricity that converts the energy from sunshine into an electric current. Solar panels, which can be used for commercial, industrial, or residential purposes, can generate more electricity by connecting several solar cells [7].

## PEROVSKITE MATERIAL

Perovskites are represented by the formula ABX<sub>3</sub>, where “A” and “B” are cations and “X” is an anion. The crystal structure can vary, forming cubic, tetragonal, or orthorhombic structures depending

on environmental conditions. Perovskites possess exceptional optical absorption properties [8], including a significant absorption coefficient and a tunable bandgap, crucial for solar cell efficiency [9].

They demonstrate excellent charge transport with long diffusion lengths, ambipolar charge mobility, and high carrier mobility, essential for efficient energy conversion. Perovskites exhibit high resistance to point defects, enhancing stability and performance across various applications. Certain perovskites, particularly those containing cobalt, exhibit magnetic characteristics due to cobalt's intrinsic spin. Optical and electrical properties of perovskites can be finely adjusted through doping, involving the introduction of controlled impurities to tailor material properties to specific needs.

These materials can be roughly divided into two groups: pure inorganic perovskites, which are represented by compounds such as  $\text{PbTiO}_2$  and  $\text{CaSiO}_2$ , and hybrid organic-inorganic perovskites, which are represented by compositions like  $\text{CH}_3\text{NH}_3\text{MX}_3$  (where  $\text{M} = \text{Pb}$  or  $\text{Sn}$ ;  $\text{X} = \text{I}$ ).

### FABRICATION OF PEROVSKITE SOLAR CELL

The “planar heterogeneous junction” structure and perovskite photovoltaic cells (PSCs) have similar designs. The ETL is made of silicon dioxide ( $\text{TiO}_2$ ), while the glass substrate layer consists of transport conducting oxides (TCO). In perovskite materials,  $\text{CuI}$  functions as the HTL for the metal back contact, and  $\text{CH}_3\text{NH}_3\text{PbI}_3$ ,  $\text{X}=\text{I}$ , serves as the active layer [10]. Fabrication of solar cell using perovskite material shown in Figure 1.

Photovoltaic cells harness the photovoltaic effect to generate electricity directly from sunlight, offering a clean energy solution that avoids emitting gases like carbon dioxide or other pollutants such as sulfur or nitrogen. Solar cells can also convert solar energy indirectly, initially transforming it into heat or chemical energy, thereby posing minimal environmental and human health risks. These cells are characterized by their low-maintenance, durability, and ease of installation in diverse settings, including homes, workplaces, caravans, tourist attractions, calculators, watches, light meters, and cameras. They provide an affordable, efficient, and environmentally friendly power source that is non-polluting, non-intrusive, and operates silently.

Global warming poses a severe threat to both humanity and wildlife on Earth [11]. Over the 19th century, sea levels rose by 10 to 25 cm, and surface temperatures increased by 0.3 to 0.6 degrees Celsius as a result of global warming. These changes in climate have led to more frequent and severe natural disasters, causing significant disruptions to human life and ecosystems.

Solar panels consist of numerous small cells designed to generate a specific amount of power. Current solar cell technologies focus on creating electrons and holes within each cell.  $\text{Cu}_2\text{O}$  serves as the HTL for the metal back contact, while  $\text{CH}_3\text{NH}_3\text{PbI}_3$ , a perovskite material, forms the active layer. The use of  $\text{Cu}_2\text{O}$  as the HTL in perovskite solar cells has been shown to enhance their efficiency [12]. Research indicates that spiro-MeOTAD exhibits a higher fill factor (FF) but lower electrical conductivity compared with  $\text{Cu}_2\text{O}$  [13].

Black metal contact
Hole transport layer (0.300 $\mu\text{m}$ )
Absorber layer ( $\text{CH}_3\text{NH}_3\text{PbX}_3$ , $\text{X}: \text{I}$ ) (0.35 $\mu\text{m}$ )
Electron transport layer (0.020, 0.030, and 0.040 $\mu\text{m}$ )
Transparent conducting oxide (0.500 $\mu\text{m}$ )
Glass substrate

**Figure 1.** Fabrication of solar cell using perovskite material.

The impressive PCE of 16.6% achieved by Cu<sub>2</sub>O-based PSCs, exceeding the median PCE of 15.6%, is likely due to the high hole mobility of the Cu<sub>2</sub>O HTL. The low surface roughness and interface resistance of the resulting perovskite films also contributed to this efficiency. Furthermore, specially designed methods have effectively reduced the degradation of the perovskite layer caused by the synthesis of Cu<sub>2</sub>O in the n-i-p PSC solution, where the active layer is CH<sub>3</sub>NH<sub>3</sub>PbI<sub>3</sub>, X = I.

## RESULTS AND DISCUSSION

The study focuses on analyzing the performance of CH<sub>3</sub>NH<sub>3</sub>PbI<sub>3</sub> perovskite solar cells under different illumination conditions, utilizing Cu<sub>2</sub>O as the HTL [14]. Key parameters such as short-circuit current density ( $J_{sc}$ ), fill factor (FF), open-circuit voltage ( $V_{oc}$ ), capacitance-frequency (C-F), capacitance-voltage (C-V), and PCE are thoroughly investigated and documented in Table II. The research highlights variations in outcomes compared to previous studies, particularly noting the cell's voltage characteristics of 0 volts in darkness and 0.5 volts under light exposure [15–20].

The variously computed characteristics of the perovskite solar cell under study (CH<sub>3</sub>NH<sub>3</sub>PbX<sub>3</sub>, X: I) shown in Table 2. For the CH<sub>3</sub>NH<sub>3</sub>PbX<sub>3</sub> (X: I) perovskite solar cell, the current density (JV) characteristics were calculated as seen in Figure 2.

**Table 2.** The variously computed characteristics of the perovskite solar cell under study (CH<sub>3</sub>NH<sub>3</sub>PbX<sub>3</sub>, X: I).

ETL Layer	Parameter			
	$V_{oc}(V)$	$J_{sc}(mAcm^{-2})$	FF	PCE (%)
At thickness 0.020 $\mu m$	2.79	26.53	41.69	30.95
At thickness 0.030 $\mu m$	2.80	26.50	41.62	30.93
At thickness 0.040 $\mu m$	2.80	26.48	41.60	30.95

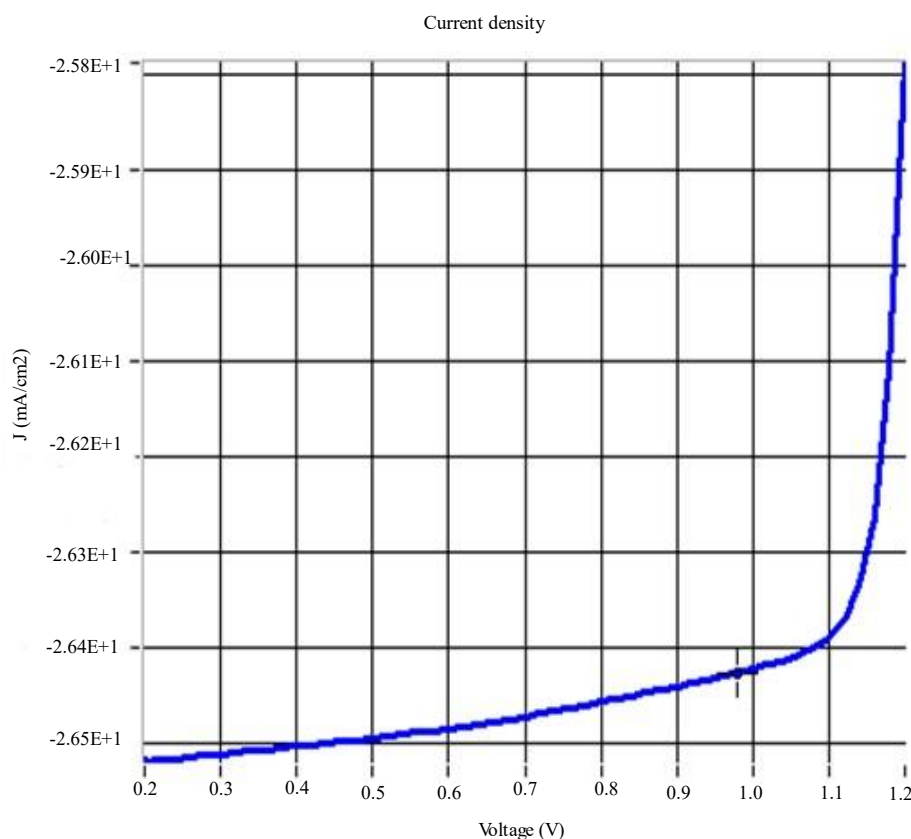


**Figure 2.** The J-V characteristics for the CH<sub>3</sub>NH<sub>3</sub>PbI<sub>3</sub> perovskite solar cell at thickness 0.020 of ETL.

Comparing the  $\text{CH}_3\text{NH}_3\text{PbI}_3$  perovskite solar cell to those of other researchers [21], at the ETL layer thickness of 0.020 micrometer the simulated findings show parameters for performance such  $V_{oc} = 2.79$ ,  $J_{sc} = 26.53$ ,  $FF = 41.69$ , and  $PCE = 30.95$  [22].

At the ETL layer thickness of 0.030 micrometer the simulated findings show parameters for performance such  $V_{oc} = 2.80$ ,  $J_{sc} = 26.53$ ,  $FF = 41.62$ , and  $PCE = 30.93$ . Also, at the ETL layer thickness of 0.040 micrometer the simulated findings show parameters for performance such  $V_{oc} = 2.80$ ,  $J_{sc} = 26.48$ ,  $FF = 41.60$ , and  $PCE = 30.95$ .

Furthermore, Figure 3 and graphs show all the output for the provided parameters by varying the thickness of the ETL with  $\text{Cu}_2\text{O}$  as an HTL. For the  $\text{CH}_3\text{NH}_3\text{PbX}_3$  (X: I) perovskite solar cell, the quantum effectiveness (QE) characteristics were calculated and plotted for an absorption coefficient of  $10^7 \text{ cm}^{-1}$ , as seen in Figure 3. For the  $\text{CH}_3\text{NH}_3\text{PbI}_3$  perovskite solar cell under study, the capacitance-frequency (C-f) properties have been determined and are displayed in Figure 4.

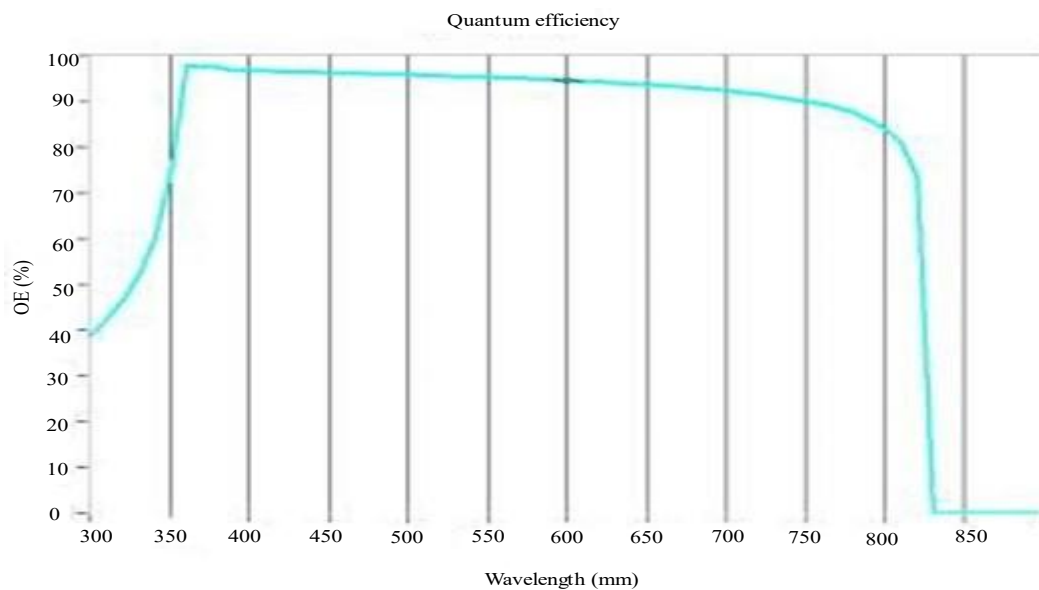


**Figure 3.** Quantum efficiency of CH NH PbI perovskite solar.

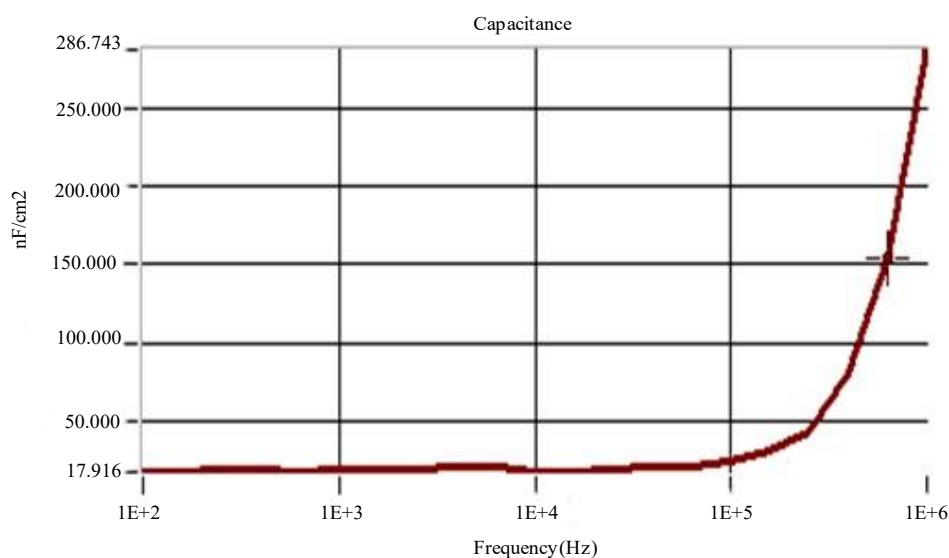


**Figure 4.** C-f characteristics for  $\text{CH}_3\text{NH}_3\text{PbI}_3$  perovskite solar cell at thickness 0.020 of ETL.

By adjusting the alternating current signal frequency during the C-f measurements, capacitance is computed. This demonstrates that  $\text{CH}_3\text{NH}_3\text{PbI}_3$  is more responsive to capacitance production at higher frequency ranges.

For a  $\text{CH}_3\text{NH}_3\text{PbI}_3$  based solar cell, the variation in capacitance ( $\text{nFcm}^{-2}$ ) is measured according to the applied voltage, and it increases exponentially with respect to voltage. For  $\text{CH}_3\text{NH}_3\text{PbI}_3$ , the capacitance ( $\text{nFcm}^{-2}$ ) rises and becomes saturated. Figure 5 plots the calculated capacitance (C) versus voltage (V) for the perovskite solar cell under investigation [23].

For the  $\text{CH}_3\text{NH}_3\text{PbX}_3$  (X: I) perovskite solar cell, the current density (JV) characteristics at thickness 0.200 of HTL were calculated as seen in Figure 6.

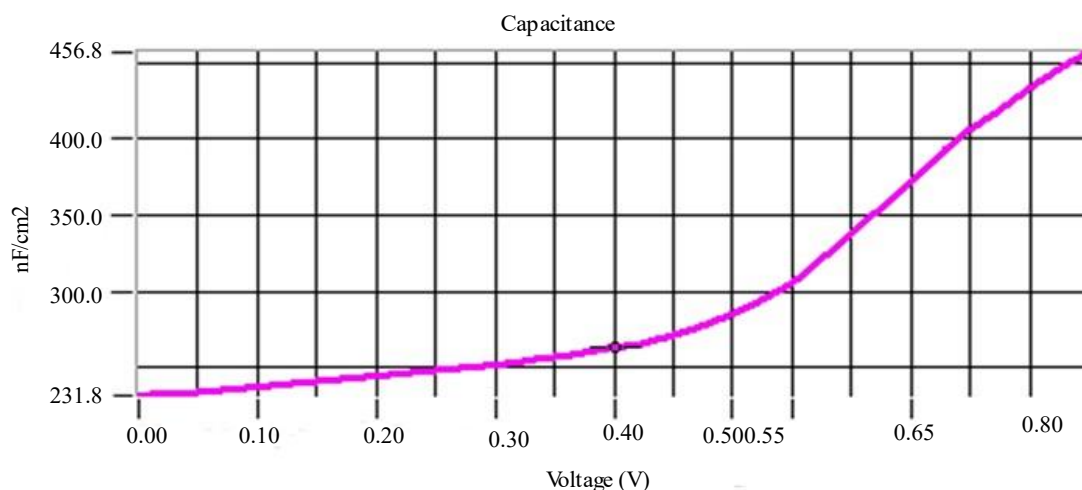


**Figure 5.** The C-V characteristics of  $\text{CH}_3\text{NH}_3\text{PbI}_3$  perovskite solar cell at thickness 0.020 of ETL333 cell at thickness 0.020 of ETL.

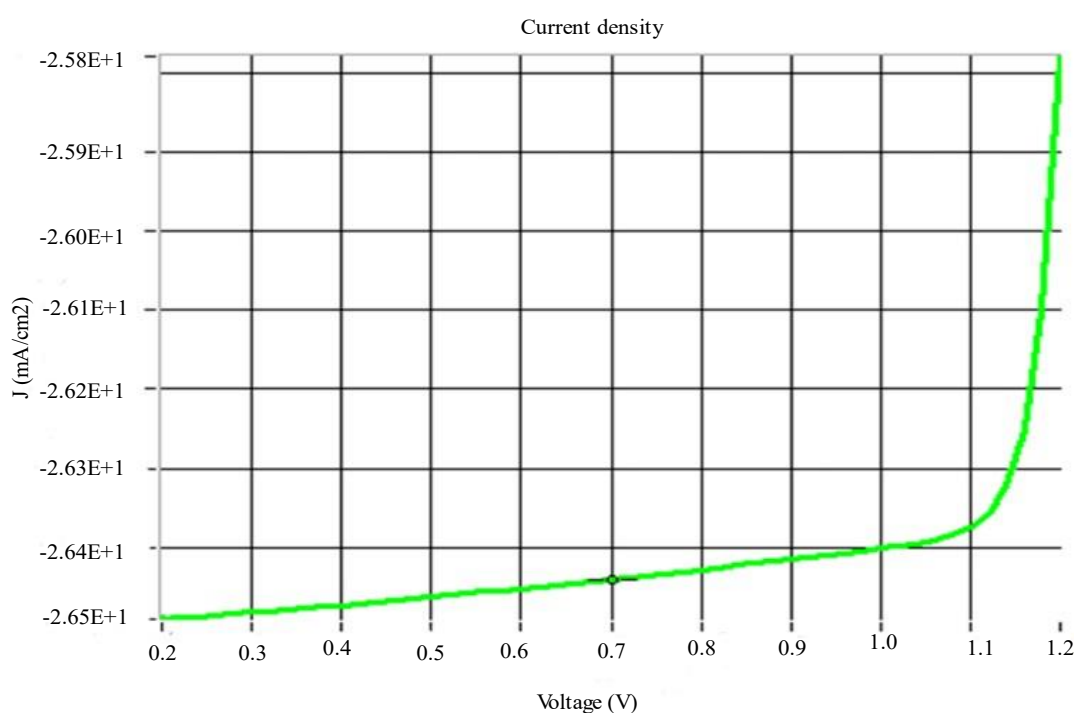


**Figure 6.** The J-V characteristics for the  $\text{CH}_3\text{NH}_3\text{PbI}_3$  perovskite solar cell at ETL thickness 0.030  $\mu\text{m}$ .

For the  $\text{CH}_3\text{NH}_3\text{PbX}_3$  (X: I) perovskite solar cell, the QE characteristics were calculated and plotted for an absorption coefficient of  $10^7$  ( $\text{cm}^{-1}$ ), as seen in Figure 7 at thickness 0.030 of ETL. For the  $\text{CH}_3\text{NH}_3\text{PbI}_3$  perovskite solar cell under study, the capacitance-frequency (C-f) properties have been determined and are displayed in Figure 8 at thickness 0.030 of ETL. By adjusting the alternating current signal frequency during the C-f measurements, capacitance is computed [24, 25]. This demonstrates that  $\text{CH}_3\text{NH}_3\text{PbI}_3$  is more responsive to capacitance production at higher frequency ranges.

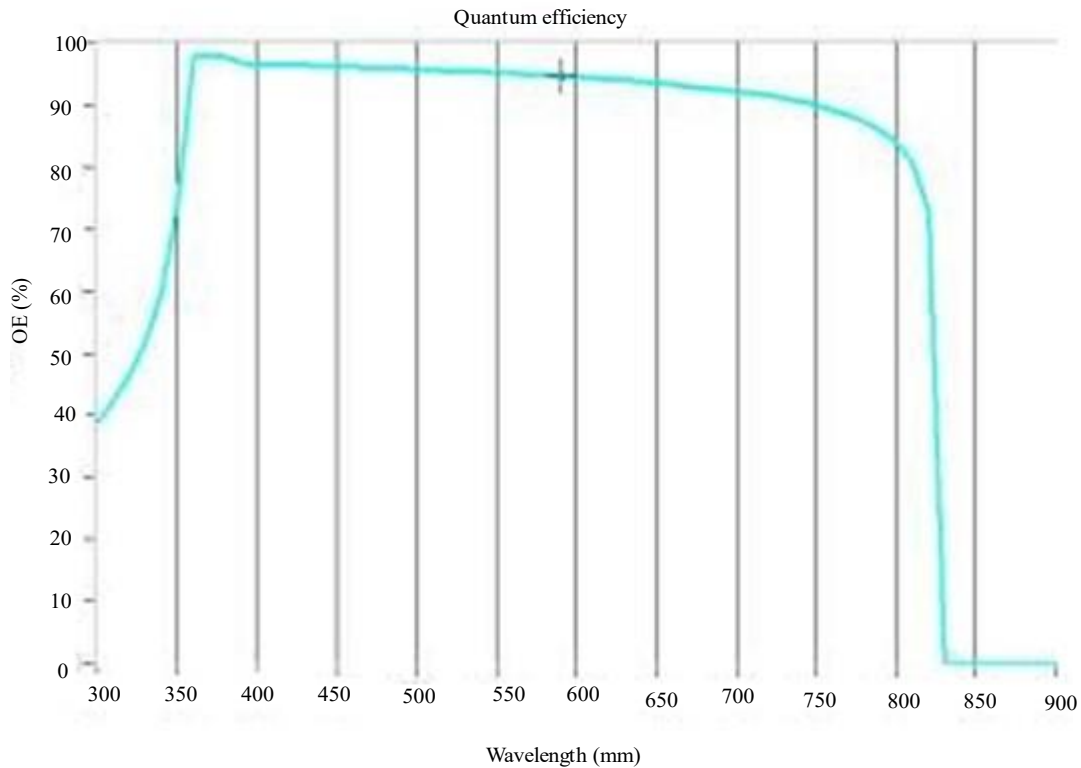


**Figure 7.** Quantum efficiency of  $\text{CH}_3\text{NH}_3\text{PbI}_3$  perovskite solar cell at ETL thickness  $0.030 \mu\text{m}$ .

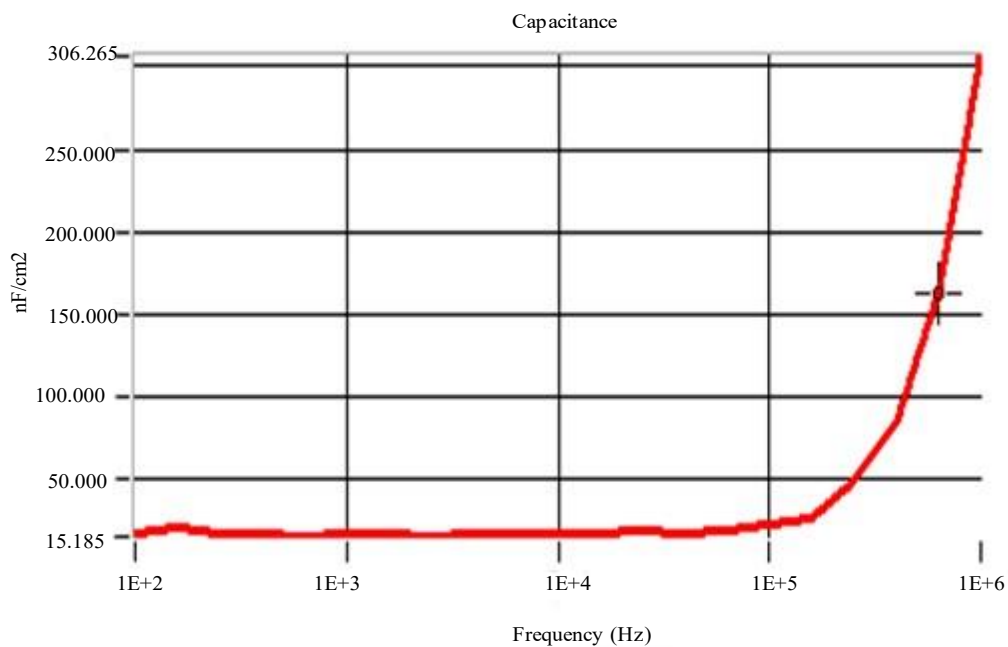


**Figure 8.** C-f characteristics for  $\text{CH}_3\text{NH}_3\text{PbI}_3$  perovskite solar cell at ETL thickness  $0.030 \mu\text{m}$ .

For a  $\text{CH}_3\text{NH}_3\text{PbI}_3$  based solar cell, the variation in capacitance ( $\text{nFcm}^{-2}$ ) is measured regarding the applied voltage, and it increases exponentially with respect to voltage at thickness 0.030 of ETL.

For  $\text{CH}_3\text{NH}_3\text{PbI}_3$ , the capacitance ( $\text{nFcm}^{-2}$ ) rises and becomes saturated. Figure 9 plots the calculated capacitance (C) vs voltage (V) for the perovskite solar cell under investigation.

For the  $\text{CH}_3\text{NH}_3\text{PbX}_3$  (X: I) perovskite solar cell, the current density (JV) characteristics were calculated as seen in Figure 10 at thickness 0.040 of ETL.

For the  $\text{CH}_3\text{NH}_3\text{PbX}_3$  (X: I) perovskite solar cell, the QE characteristics were calculated and plotted for an absorption coefficient of  $10^7$  ( $\text{cm}^{-1}$ ), as seen in Figure 11 at thickness 0.040 of ETL.

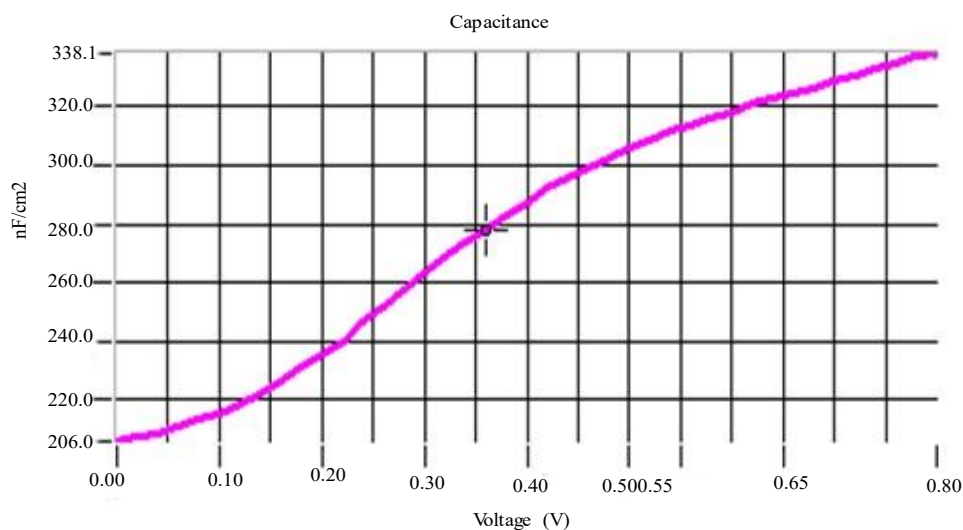


**Figure 9.** The C-V characteristics of  $\text{CH}_3\text{NH}_3\text{PbI}_3$  perovskite solar cell at ETL thickness 0.030  $\mu\text{m}$ .

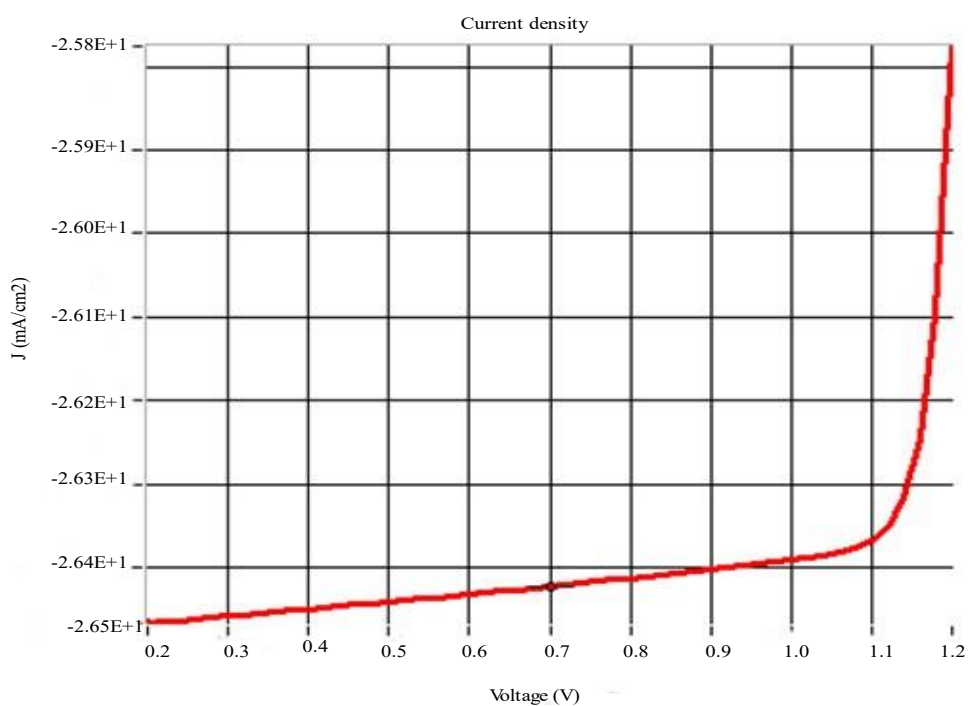


**Figure 10.** The J-V characteristics for the  $\text{CH}_3\text{NH}_3\text{PbI}_3$  perovskite solar cell at ETL thickness 0.040  $\mu\text{m}$ .

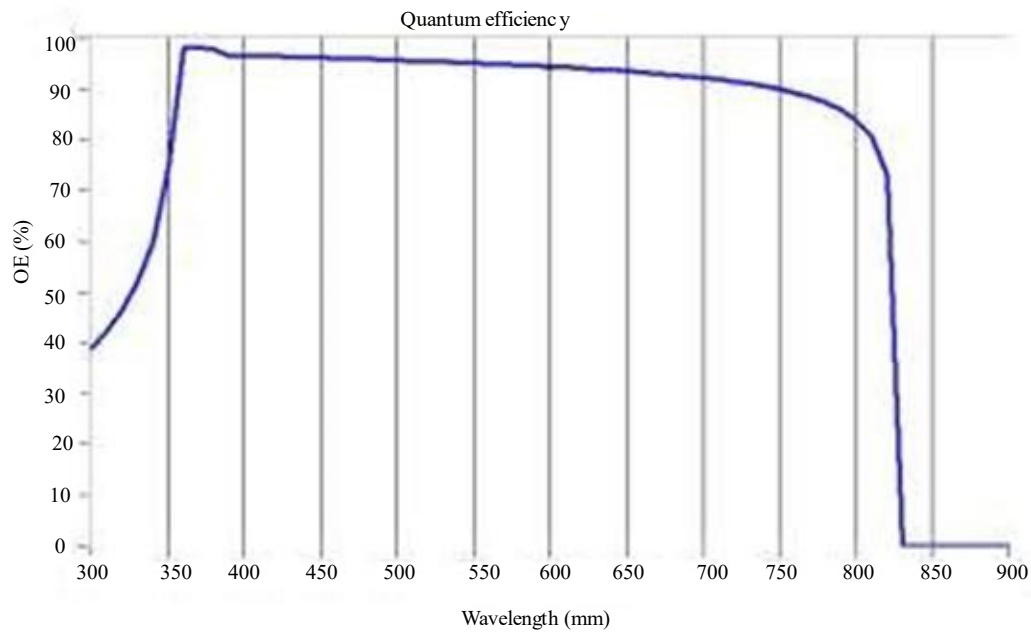


**Figure 11.** Quantum efficiency of  $\text{CH}_3\text{NH}_3\text{PbI}_3$  perovskite solar cell at ETL thickness  $0.040 \mu\text{m}$ .

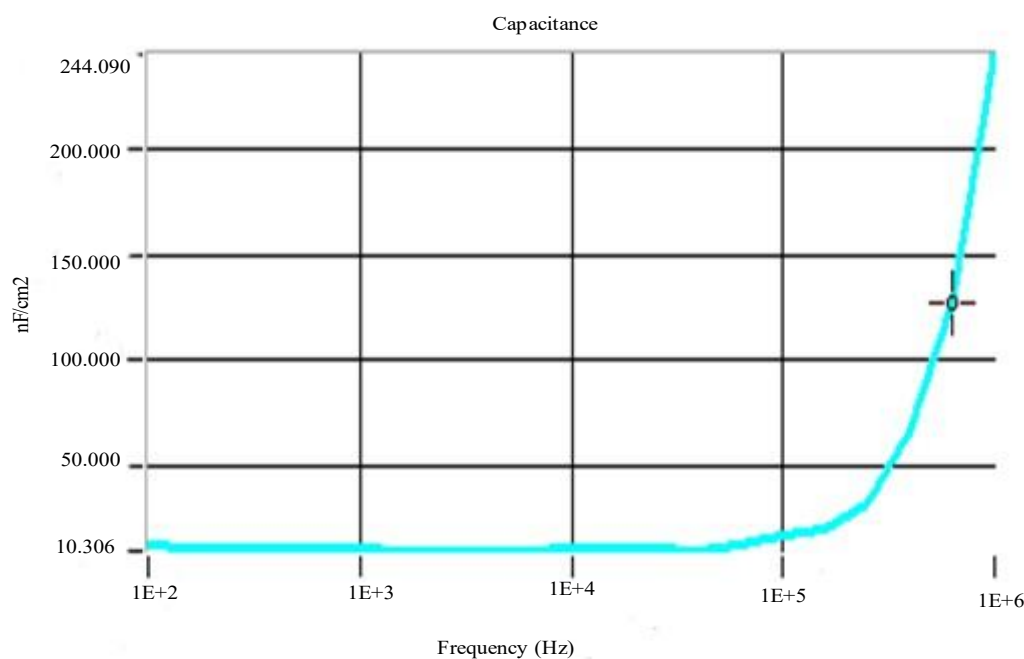


**Figure 12.** C-f characteristics for  $\text{CH}_3\text{NH}_3\text{PbI}_3$  perovskite solar cell at ETL thickness  $0.040 \mu\text{m}$ .

For the  $\text{CH}_3\text{NH}_3\text{PbI}_3$  perovskite solar cell under study, the capacitance-frequency (C-f) properties have been determined and are displayed in Figure 12 at thickness  $0.040 \mu\text{m}$  of ETL. By adjusting the alternating current signal frequency during the C-f measurements, capacitance is computed. This demonstrates that  $\text{CH}_3\text{NH}_3\text{PbI}_3$  is more responsive to capacitance production at higher frequency ranges.

For a  $\text{CH}_3\text{NH}_3\text{PbI}_3$  based solar cell, the variation in capacitance ( $\text{nFcm}^{-2}$ ) is measured regarding the applied voltage, and it increases exponentially with respect to voltage at thickness  $0.040 \mu\text{m}$  of ETL. For  $\text{CH}_3\text{NH}_3\text{PbI}_3$ , the capacitance ( $\text{nFcm}^{-2}$ ) rises and becomes saturated. Figure 13 plots the calculated capacitance (C) vs voltage (V) for the perovskite solar cell under investigation.

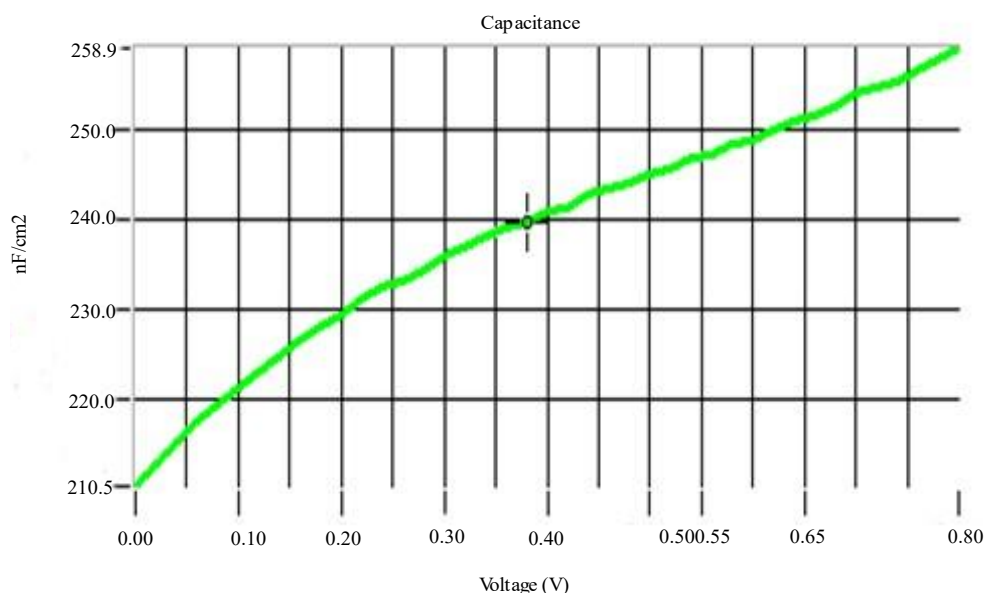


**Figure 13.** The C-V characteristics of  $\text{CH}_3\text{NH}_3\text{PbI}_3$  perovskite solar cell at ETL thickness  $0.040 \mu\text{m}$ .

## CONCLUSION

This study emphasizes the critical role of the HTL in enhancing the efficiency of solar cells using perovskite materials like  $\text{CH}_3\text{NH}_3\text{PbI}_3$ , analyzed through the SCAPS (Solar Cell Capacitance Simulator) tool. Quantitative simulations and modeling were employed to assess the electrical characteristics of the  $\text{MAPbI}_3$  material in the active layer, focusing on parameters such as fill factor (FF), short-circuit current density ( $J_{sc}$ ), PCE, and open-circuit voltage ( $V_{oc}$ ). Additionally, calculations were conducted for capacitance-frequency (C-F) and capacitance-voltage (C-V) characteristics of previously studied perovskite solar cells.

Simulation results indicate that varying the thickness of the ETL impacts the performance metrics of  $\text{MAPbI}_3$  perovskite solar cells: At an ETL thickness of  $0.020 \mu\text{m}$ , the solar cells exhibited  $\text{FF} = 41.69\%$ ,  $\text{PCE} = 30.95\%$ ,  $V_{oc} = 2.79\text{V}$ , and  $J_{sc} = 26.53 \text{ mA/cm}^2$ . At  $0.030 \mu\text{m}$  thickness, the metrics were  $\text{FF} = 41.62\%$ ,  $\text{PCE} = 30.93\%$ ,  $V_{oc} = 2.80\text{V}$ , and  $J_{sc} = 26.80 \text{ mA/cm}^2$ . At  $0.040 \mu\text{m}$  thickness, the results were  $\text{FF} = 41.60\%$ ,  $\text{PCE} = 30.95\%$ ,  $V_{oc} = 2.80\text{V}$ , and  $J_{sc} = 26.48 \text{ mA/cm}^2$ .

## REFERENCES

- Swami R. Solar cell. *Int J Sci Res Publ.* 2012; 2 (7): 1.
- Sharma S, Jain KK, Sharma A. Solar cell: In research and application: a review. *Mater Sci Appl.* 2015; 6: 1145–1155. Doi: 10.4236/msa.2015.612113.
- Tiwari T. (2018). Next generation solar power technology. [Online] Available at [www.electronicsforu.com](http://www.electronicsforu.com) [Accessed on September 2024]
- Taghavi J, Houshmand M, Zandi MH, Gorji NE. Modeling of optical losses in perovskite solar cells. *Sol Energy Mater Sol Cells.* 2016; 149: 424–428. Doi: 10.1016/j.solmat.2015.09.038.
- Pandey R, Chaujar R. Numerical simulations: Toward the design of 27.6% efficient four-terminal semi-transparent perovskite/SiC passivated rear contact silicon tandem solar cell. *Sol Energy Mater Sol Cells.* 2016; 100: 656–666. Doi: 10.1016/j.solmat.2015.12.023.
- Kibria MT, Ahammed A, Sony SM, Hossain F, Islam SU. Comparative studies on different generation solar cells technology. In: *Proceedings of the International Conference on Environmental Aspects of Bangladesh (ICEAB); 2014 September 13–14; Dhaka, Bangladesh: ICEAB.* Available at <https://warstek.wordpress.com/wp-content/uploads/2015/05/comparative-studies-on-different-generation-solar-cells-technology.pdf> [Accessed on September 2024]
- Ranabhat K, Patrikeev L, Andrianov K, Lapshinsky V, Sofronova E. An introduction to solar cell technology. *Int J Renew Energy Res.* 2016; 4 (4): 481–491.

8. Chen CW, Hsiao SY, Chen CY, Kang HW, Huang ZY, Lin HW. Optical properties of organometal halide perovskite thin films and general device structure design rules for perovskite single and tandem solar cells. *J Mater Chem A*. 2015; 3 (17): 9152–9159. Doi: 10.1039/C4TA06465A.
9. Huang ZL, Chen CM, Lin ZK, Yang SH. Efficiency enhancement of regular-type perovskite solar cells based on Al-doped ZnO nanorods as electron transporting layers. *Sol Energy Mater Sol Cells*. 2017; 102: 94–102. Doi: 10.1016/j.solmat.2016.12.004.
10. Yang WS, Noh JH, Jeon NJ, Kim YC, Ryu S, Seo J, Seok SI. High-performance photovoltaic perovskite layers fabricated through intra-molecular exchange. *Science*. 2015; 348 (6234): 1234–1237. Doi: 10.1126/science.aaa9272.
11. Hosenuzzaman M, Rahim NA, Selvaraj J, Hasanuzzaman M, Malek ABM, Nahar A. Global prospects, progress, policies, and environmental impact of solar photovoltaic power generation. *Renew Sustain Energy Rev*. 2015; 41: 284–297. Doi: 10.1016/j.rser.2014.10.027.
12. Kumar P, Babu G. Recent advances in perovskite-based solar cells. *Curr Sci*. 2016; 111 (7): 1173–1181.
13. Wu N, Wu Y, Walter D, Shen H, Duong T, Grant D, et al. Identifying the cause of voltage and fill factor losses in perovskite solar cells by using luminescence measurements. *Energy Technol*. 2017; 5 (11): 2151–2160. Doi: 10.1002/ente.201700374.
14. Verschraegen J, Burgelman M. Numerical modeling of intra-band tunneling for heterojunction solar cells in SCAPS. *Thin Solid Films*. 2007; 515 (15): 6276–6279. Doi: 10.1016/j.tsf.2006.11.158.
15. Masuko K, Shigematsu M, Hashiguchi T, Fujishima D, Kai M, Yoshimura N, et al. Achievement of more than 25% conversion efficiency with crystalline silicon heterojunction solar cell. *IEEE J Photovoltaics*. 2016; 6 (6): 1433–1435. Doi: 10.1109/JPHOTOV.2016.2602841.
16. Wehrenfennig C, Eperon GE, Johnston MB, Snaith HJ, Herz LM. High charge carrier mobilities and lifetimes in organolead trihalide perovskite. *Adv Mater*. 2014; 26 (10): 1584–1589. Doi: 10.1002/adma.201305172.
17. Bottaro C, Moscovitz A. Current photovoltaic technology: Current progress and future prospects. MIT-EL77-041W. Cambridge, MA, USA: Massachusetts Institute of Technology; 1997.
18. Homes CC. Optical response of high dielectric-constant perovskite-related oxide. *Science*. 2001; 293 (5530): 673–676. Doi: 10.1126/science.1063445.
19. Sadeghi F, Neghabi M. Optimization of structure of solar cells based on lead-based perovskite via numerical simulation. *J Sol Energy Res*. 2017; 24 (4): 315–321.
20. Jeng JY, Chiang YF, Lee MH, Peng SR, Guo TF, Chen P, Wen TC. CH<sub>3</sub>NH<sub>3</sub>PbI<sub>3</sub> perovskite/fullerene planar-heterojunction hybrid solar cells. *Adv Mater*. 2013; 25 (27): 3727–3732. Doi: 10.1002/adma.201301327.
21. Miyazawa Y, Ikegami M, Chen HW, Ohshima T, Imaizumi M, Hirose K, Miyasaka T. Tolerance of perovskite solar cells to high-energy particle irradiations in space environment. *iScience*. 2018; 2: 148–155. Doi: 10.1016/j.isci.2018.03.021.
22. Correa-Baena JP, Abate A, Saliba M, Tress W, Jacobsson TJ, Grätzel M, Hagfeldt A. The rapid evolution of highly efficient perovskite solar cells. *Energy Environ Sci*. 2017; 10 (3): 710–727. Doi: 10.1039/C6EE03397K.
23. Haider SZ, Anwar H, Wang M. A comprehensive device modeling of perovskite solar cell with inorganic copper iodide as hole transport material. *Semicond Sci Technol*. 2018; 33 (3): 035001. Doi: 10.1088/1361-6641/aaa7b7.
24. Giordano F, Abate A, Correa Baena JP, Saliba M, Matsui T, Im SH, et al. Enhanced electronic properties in mesoporous TiO<sub>2</sub> via lithium doping for high-efficiency perovskite solar cells. *Nat Commun*. 2016; 7: 10379. Doi: 10.1038/ncomms10379.
25. Chen D, Zhang C. Interface engineering and electrode engineering for organic solar cells. In: Ali K, editor. *Organic solar cells: advances and developments*. Rijeka, Croatia: InTechOpen; 2016. Doi: 10.5772/65312.